A Multi-Scale Topo-Morphologic Approach for Separating Arteries and Veins in Pulmonary CT Images

Punam Kumar Saha[1,2], Milan Sonka[1], Zhiyun Gao[1], Eric Hoffman[2]

[1]Depts. of Electrical & Computer Engineering, and [2]Radiology
The University of Iowa, Iowa City, IA 52242

Abstract. In this paper, we present a new method for separating two iso-intensity objects attached to each other at different locations at various scales and apply the method to separating arteries and veins in pulmonary CT images. The method starts with two sets of seeds — one for arteries and another for veins. Initialized with seeds, arteries and veins grow iteratively while maintaining their spatial separation and eventually forming two disjoint objects at convergence. The method combines fuzzy distance transform, a morphologic feature, with a topologic connectivity property to iteratively separate finer and finer details starting at a large scale and progressing towards smaller scales. The method has been validated in mathematically generated tubular objects with different levels of fuzziness, scale and noise. Also, it has been successfully applied to *in vivo* clinical CT pulmonary data for separating arteries and veins. Results have demonstrated the method's ability to resolving multi-scale adherence of two iso-intensity objects even when there are no sign of intensity variation at conjoining locations.

1 Introduction

Image Segmentation [8] – a method of producing a spatio-temporal object definition in an image – has remained a salient task in most medical imaging applications. Different segmentation methods [3] focus on different image features and properties and often, the design of an effective segmentation algorithm in a limited SNR and resolution regime is highly challenging and application dependent. Here, we have selected a specific segmentation task of separating arteries and veins (*A/V*) via *in vivo* pulmonary CT imaging with no blood pool enhancing contrast. Although, such a method of separating A/V is very useful, the challenges are multi-folded including — (1) A/V are indistinguishable by their intensity values in non-contrast pulmonary CT images, (2) often, there is no trace of intensity variation at locations of adherence between A/V, (3) complex and tight coupling between A/V with arbitrary and multi-scale geometry, especially, at branching locations and (4) limited SNR and resolution of *in vivo* imaging. Patient-specific structural abnormalities of vascular trees further complicate the task. Several works have been reported in literature toward solving the problems of separating arteries and veins using improvised image acquisition techniques; a thorough discussion on difficulties of such approaches, especially, for smaller vessels has been presented by Bemmel *et al* [10]. As far as our knowledge goes, only a few post-processing methods have been published on separating arteries and veins [2,10]. The previous methods have been applied to MR data only and do not use morphological scale information.

These methods primarily rely on intensity variation or edge information at the adherence locations between A/V and may not work for *in vivo* CT images where no intensity variations are visible at locations of adherence between A/V. Recently, two approaches for artery/vein classification from pulmonary CT images appeared [1,11].

Here, we introduce the use of morphologic scale features which enables separating two structures even when there is no edge feature at locations of adherence between the two which often happens between A/V in CT data. Specifically, we develop a new topo-morphologic method that iteratively separates A/V starting from two sets of seeds at high scale and then progressively solves the problem at lower scales. The method combines fuzzy topological approaches [4,9,5] with fuzzy distance transform [6] — a morphological feature — without requiring a parameter. Separated A/V trees may significantly contribute to our understanding of pulmonary structure and function and has immediate clinically applicable applications, e.g., for assessment of pulmonary emboli. The knowledge of separated A/V may significantly boost performance of airway segmentation methods.

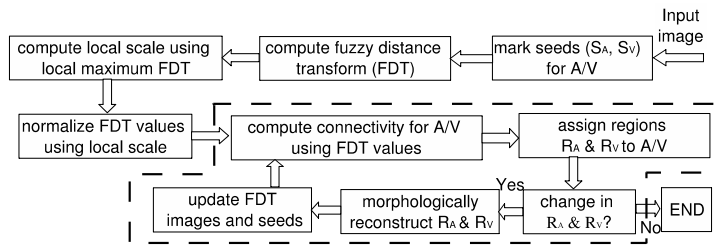

Fig. 1. A schematic description of the overall method.

2 Theory and Methods

The overall work flow diagram of the method is presented in Figure 1 that separates two iso-intensity objects using multi-scale morphological features. As input, it receives fuzzy segmentation of the assembly of two iso-intensity objects and two sets of seeds — one for each object — and it outputs separated objects. Although the method immediately extends to multiple objects, here we formulate a solution for two objects only and we will refer one object as the rival of the other. Let us consider an image consisting of two iso-intensity fuzzy objects with significant noise and overlapping as shown in Figure 2(a); a few cross sectional images are shown in Figure 2(b). The two cylinders with gradually reducing radii are running in parallel. The diameter of one cylinder is significantly larger than other; a sinusoidal swing is added to both in the xy-coordinate direction so that central lines of both cylinders lie on an xy-plane, say

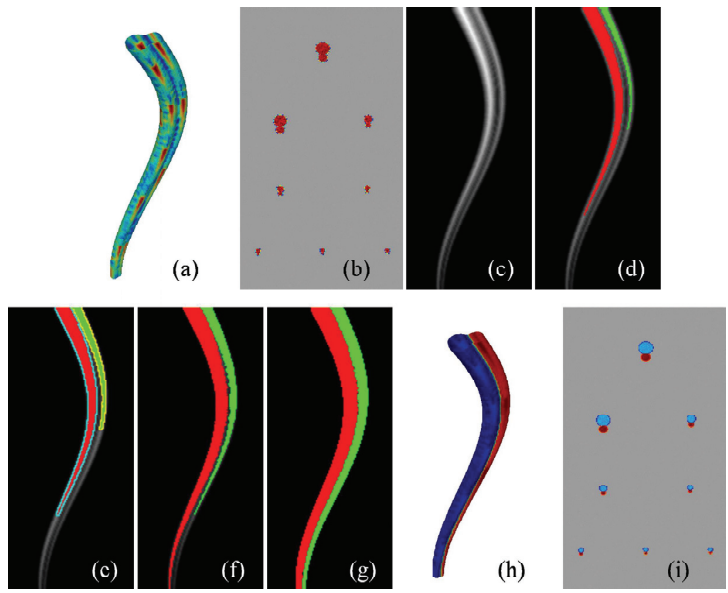

Fig. 2. (a) 3D rendition of a phantom image. (b) A few cross-sectional images. (c) FDT image on the central xy-plane. (d) Results of separation of the two cylinders after the first iteration using FDT-based connectivity. (e) Morphologic reconstruction based on the results of (d). (f,g) Same as (d) after second (f) and terminal (g) iterations. (h,i) 3D rendition and cross-sectional images of the result.

the *central xy-plane*. Usefulness of the method may be better understood in three and higher dimensions. On the other hand, it is always easier to illustrate a method in 2D. Therefore, we illustrate results of different steps of the method on the central xy-plane. One seed is manually placed through a graphical interface on the approximate center of each cylinder at the top-most cross-section. As shown in Figure 1, the process is iterative and begins with marking the seeds followed by fuzzy distance transform (FDT) computation [6] of the assembly of two cylinders prior to iterations; see Figure 2(c) for the results of FDT computation. It is visually notable from the FDT image that we cannot find a single FDT threshold to separate the two cylinders from their head to tail. Therefore, no straightforward morphological opening operator can solve the problem. On the other hand, over a small region, the two cylinders seem separable using their FDT values. In other words, the problem demands regional selection of an optimum opening structure to separate the two cylinders.

The above observation motivated us using *local scale* to normalize FDT values that reduces the effect of spatial scale variations. Local scale at a point p is defined as the FDT value of the locally-deepest point (a point with locally maximum FDT value) that is nearest to p. With the normalized FDT map, the method adopts an iterative strategy that first separates the cylinders over large-scale regions using FDT-based relative connectivity [5] where a point is grabbed by an object if its connectivity to the point is strictly greater than that of its rival. A separator is built between the two objects using a morphological reconstruction method that simultaneously and radially dilates each currently segmented region until blocked by its rival (maximum radius of the dilating structure is determined by FDT values). Figures 2d & e show the results of initial separation and morphologic reconstruction of two cylinders after first iteration. In the next iteration, the FDT-connectivity paths of one object are not allowed to enter into the region assigned to its rival. This strategy facilitate resolving fusion at smaller scale regions (Figure 2f) and this iterative process is continued as long as there is any change. For this phantom image, the method stopped after 12 iterations (see Figure 2g–i for final separation).

3 Results and Discussion

Effectiveness of the method has been examined by applying it to mathematically generated phantoms and to clinical CT pulmonary images. Five mathematical phantoms were computer-generated as tubular objects running across the slice direction with different levels of fuzziness, overlap, scale and noise. Initially, the phantom images were generated at high resolution and then downsampled using 3×3×3, 4×4×4 and 5×5×5 windows. Each downsampled image was degraded with additive noise at SNR of 12. Using a graphical interface, exactly one seed point was manually selected for each tubular object in a phantom near its center on the slice at the lower-most level. Although there is no thoretical restriction on positioning the seed points, the seeds are were positioned close to the vessel centerlines. Phantoms and results are depicted in Figure 3 at $4\times4\times4$ and $5\times5\times5$ downsampling only, as the method has always successfully separated the two cylinders at $3\times3\times3$ downsampling. At extremely low resolution and high noise, the morphological information may be entirely lost, leading to a failure of separation

in Figure 3t,v. Specifying another pair of seeds would be help achieving correct separation. Cross sectional images of the first phantom are illustrated at both resolutions to depict the 3D phantom image quality used and the complexity of separating the two objects. The smallest radius of the phantom of Figure 3a is 1.87 pixels at the downsampling by $4 \times 4 \times 4$ pixels; the largest radius in the same example at same downsampling resolution is 18.75 pixels. Except for the examples of Figures 3a and f, the radii of the two cylinders differed significantly.

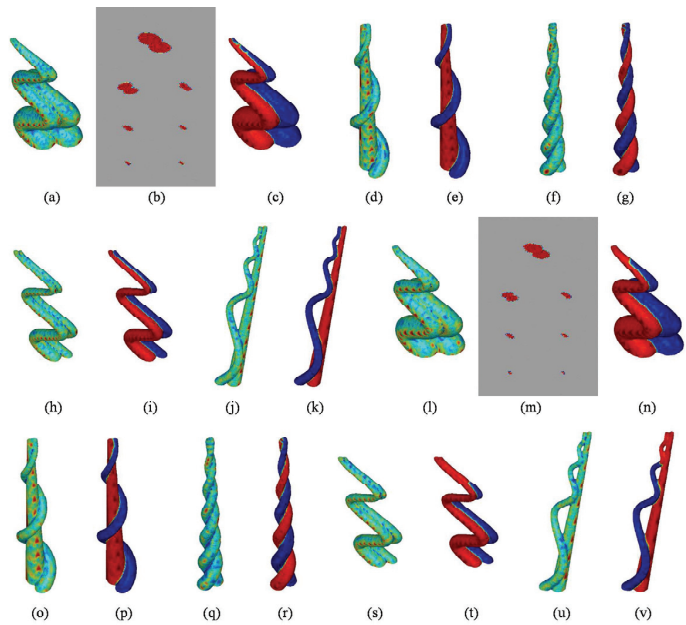

Fig. 3. (a-k) Results of our method's application to several 3D phantom images downsampled by $4 \times 4 \times 4$. (a,b) 3D rendition and cross-sectional images of one phantom image. (c) Separated cylinders. (d-k) Results for other four phantoms. (l-v) Results of application of the method at downsampling by $5 \times 5 \times 5$.

The method has been applied to separate arteries and veins in pulmonary CT images (see Figure 4). Thoracic region of two females of age 22 Y and 27 Y were scanned using a Siemens Sensation 64 MDCT scanner at 120 kVp and 200 mAs. One subject was scanned in feet first supine while the other was scanned in head first supine position.

Images were acquired at 0.75 mm slice thickness and were reconstructed with 0.5 mm slice-thickness and 0.55x0.55 mm^2 in-plane resolution. Entire vascular tree of both lungs was segmented in each CT image data using the method of Shikata *et al.* [7] that uses tree-connectivity on the CT intensity image enhanced by the output of a tubular enhancement filter. Resulting A/V separation outcomes are shown in Figure 4. Seed points were manually selected using a 2D slice-display graphical interface followed by the application of the morphological separator algorithm. The subsequent automated process requires 2 to 3 mins. to complete the A/V separation for the right or left lung. Finally, the separated A/V were displayed with color coding (red for veins and blue for arteries; see Figures 4b,c) through a 3D surface rendition software tool developed in-house using VTK-based 3D visualization filter classes.

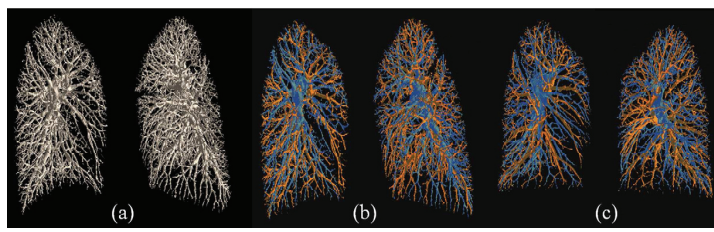

Fig. 4. Results of application to pulmonary CT images. (a) 3D surface renditions of vessel trees in left and right lungs. (b) Color-coded 3D rendition of separated artery/vein trees. (c) Same as (b) but for another dataset. Blue – arteries (carrying non-oxygenated blood), red – veins.

The method has demonstrated feasibility of separating two iso-intensity structures with multi-scale adherences even when there is no sign of intensity-based separation at joining locations. The method seeks morphological identities of each object at a specific scale and separates them without using any gradient- or edge-like features. Introduction of the ideas of morphological reconstruction and separator allows the method to seal the joining border at current scale and then seek morphological features identifying different objects at finer scales. The mathematical phantom demonstrates the ability of the method when the geometry of coupling of two objects are known and its performance with just one seed for each object is encouraging. For pulmonary CT images, the geometry of coupling between arteries and veins are far more challenging and quite unknown. However, the method has shown acceptable performance with a reasonable number of seeds. Approximately 25–35 seeds were manually selected on each of the A/V subtrees. It may be pointed out that the seeds were selected using a 2D graphical tool. Often multiple seeds were placed within the same locality of an object and therefore, not all of the seeds contributed to true A/V separation. We have found that seed selection is an important task in the entire process and the current seed-selection tool is

far from optimal. An effective seed selection process must be performed through a 3D graphical interface coupled with the morphological separator providing a transparent interactive environment to the user. Currently, we are developing such a seed-selection graphical system and we believe that, once it is developed, the number of seeds required will significantly decrease.

Acknowledgments This work has been partially supported by the NIH grant RO1 HL-064368. The authors wish to thank Dr. Guoyuan Liang and Ms. Yan Xu for their helps in generating the color display of Figure 4.

References

1. T. Buelow, R. Wiemker, T. Blaffert, C. Lorenz, and S. Renisch. Automatic extraction of the pulmonary artery tree from multi-slice ct data. In *Proceedings of SPIE: Medical Imaging*, volume 5746, pages 730–740, San Diego, CA, 2005. 2
2. T. Lei, J. K. Udupa, P. K. Saha, and D. Odhner. Artery-vein separation via MRA - an image processing approach. *IEEE Transactions on Medical Imaging*, 20:689–703, 2001. 1
3. D. Pham, X. Chenyiang, and J. L. Prince. A survey of current methods in medical image segmentation. *Annual Review of Biomedical Engineering*, 2:315–337, 2000. 1
4. A. Rosenfeld. Fuzzy digital topology. *Information and Control*, 40:76–87, 1979. 2
5. P. K. Saha and J. K. Udupa. Iterative relative fuzzy connectedness and object definition: theory, algorithms, and applications in image segmentation. In *Proceedings of IEEE Workshop on Mathematical Methods in Biomedical Image Analysis*, Hilton Head, South Carolina, 2000. 2, 4
6. P. K. Saha, F. W. Wehrli, and B. R. Gomberg. Fuzzy distance transform - theory, algorithms, and applications. *Computer Vision and Image Understanding*, 86:171–190, 2002. 2, 4
7. H. Shikata, E. Hoffman, and M. Sonka. Automated segmentation of pulmonary vascular tree from 3D CT images. In *Proceedings of SPIE: Medical Imaging*, volume 5369, pages 107–116, San Diego, CA, 2004. 6
8. M. Sonka, V. Hlavac, and R. Boyle. *Image Processing, Analysis, and Machine Vision*. PWS Publishing, Pacific Grove, CA, 1999. 1
9. J. K. Udupa and S. Samarasekera. Fuzzy connectedness and object definition: theory, algorithms, and applications in image segmentation. *Graphical Models and Image Processing*, 58:246–261, 1996. 2
10. C. M. van Bemmel, L. J. Spreeuwers, M. A. Viergever, and W. J. Niessen. Level-set-based arteryvein separation in blood pool agent CE-MR angiograms. *IEEE Transactions on Medical Imaging*, 22:1224–1234, 2003. 1
11. T. Yonekura, M. Matsuhiro, S. Saita, M. Kubo, Y. Kawata, N. Niki, H. Nishitani, H. Ohmatsu, R. Kakinuma, and N. Moriyama. Classification algorithm of pulmonary vein and artery based on multi-slice ct image. In *Proceedings of SPIE: Medical Imaging*, volume 6514, 65142E, San Diego, CA, 2007. 2